Journal of Advanced Joining Processes 13 (2026) 100398

Contents lists available at ScienceDirect

Journal of Advanced Joining Processes

journal homepage: www.sciencedirect.com/journal/journal-of-advanced-joining-processes

Influence of post-weld heat-treatment on global and local mechanical properties of friction stir welded AA6082 and AA7050 to Ti6Al4V

Felix Grassel *, Benjamin Klusemann

Institute of Material and Process Design, Helmholtz-Zentrum Hereon, Max–Planck-Strasse 1, 21502 Geesthacht, Germany
Institute for Production Technology and Systems, Leuphana University Lüneburg, Universitätsallee 1, 21335 Lüneburg, Germany

ARTICLE INFO

Dataset link: 10.5281/zenodo.19559286

Keywords:
Aluminium
Titanium
Friction stir welding
Heat treatment
Intermetallic compounds

ABSTRACT

This study investigates the macroscopic as well as local mechanical properties of dissimilar aluminium-titanium joints obtained via friction stir welding, followed by heat treatments. For this purpose, the two widely used alloys AA6082 (AlMgSi) and AA7050 (AlCuZn) are friction-stir lap welded to Ti6Al4V. Post-weld heat-treatment between 6 and 48 h with a temperature range up to 420 °C is applied to investigate the diffusion behaviour. Besides the well-established lap-shear test, micro tensile tests were performed to investigate the local mechanical properties of the interface in the weld. Heat-treatment temperatures above 120 °C resulted in an increase of up to 40 % in strength compared to as-welded. UTS values reached up to 157 N/mm^2 and 225 N/mm^2. The diffusion kinetics of AlMgSi alloys is found to be significantly higher than that of AlCuZn alloys with Mg having the most significant influence on diffusion.

Introduction

Friction stir welding (FSW), invented in 1991 (Thomas et al., 1995), has proven to be able to join various similar and also dissimilar material combinations (Mishra and Ma, 2005) like aluminium to copper (Isa et al., 2021), steel (Beygi et al., 2023), polymers (Haghshenas and Khodabakhshi, 2019) and titanium (Simar and Avettand-Fènoël, 2017), especially, which were typically considered to be unweldable with conventional, fusion-based techniques. However, two main issues deteriorate the joint strength in dissimilar weld combinations: The difference in thermal properties, especially the solidus and evaporation temperatures as well as the formation of brittle intermetallic compounds (IMC). Both issues are particularly prominent in joining of aluminium and titanium alloys. But in recent years, dissimilar FSW of Al and Ti has made huge progress, allowing for welds that reach more than 90 % of the base material strength (Grassel et al., 2025). However, the relative and absolute values of strength depend significantly on the chemical composition of the specific aluminium alloy. For non-precipitation-hardening alloys like the 1xxx (Wei et al., 2012) and 5xxx series (Rostami et al., 2018), joint strength close to the base material are achieved, while for some precipitation-hardening alloys like the 6xxx series (Wu et al., 2015), the joint strength is limited due to material softening in the heat-affected zone (HAZ). Contradictory, when welded to Ti, other precipitation-hardening alloys like 2xxx (Dressler et al., 2009) and 7xxx (Österreicher et al., 2024) series showed fracture in the interface, implicating low absolute strength in the as-welded state.

To understand the bonding process between Al and Ti, thermo-mechanical conditions during joining and the resulting metallurgical effects have to be revealed. Yu et al. (2019) investigated the influence of energy input on the interface formation during friction stir lap-welding (FSLW) of AA6061 and Ti6Al4V and found a flat “diffusive” interface at low heat input, where Ti is not plastically deformed, and a inhomogeneous “mixed” interface at high heat input, where the Ti surface is grooved and particles are mixed into Al. They observed highest mechanical properties for parameters at the transition point between both interface morphologies. Similar results were obtained by Krutzlinger et al. (2014), varying rotational speed as well as tool to interface distance in FSLW of AA6082 and Ti6Al4V. Chen and Yazdanian (2015) made the same observation varying the probe penetration in FSLW of AA6060 to Ti6Al4V, resulting in an IMC layer of 250 nm. Kalinenko et al. (2022) used a probe tip to interface distance of 50 µm to avoid tool wear during FSLW of AA6013 and Ti6Al4V, where a high strength was achieved at relatively high heat input. On the other hand, the strength was limited as the introduced heat deteriorated the Al mechanical properties in the HAZ. In summary, for firm welding of AA6xxx alloys to Ti, a relatively high heat input is beneficial, while the strength is limited by the weakening effect of Ti flakes or softening in the HAZ of Al.

* Corresponding author at: Institute of Material and Process Design, Helmholtz-Zentrum Hereon, Max–Planck-Strasse 1, 21502 Geesthacht, Germany.
E-mail address: felix.grassel@hereon.de (F. Grassel).

https://doi.org/10.1016/j.jajp.2026.100398
Received 18 January 2026; Received in revised form 18 March 2026; Accepted 8 April 2026
Available online 10 April 2026

Table 1
Chemical composition [wt. %] and ultimate tensile strength [N/mm^2] of investigated materials. The values for the aluminium alloys were taken from charge analysis while the values for Ti6Al4V are taken from AMS 4911 and ASTM B265.

	Si	Fe	Cu	Mn	Mg	Cr	Zn	Ti	V	Al	R_m
AA6082-T6	0.93	0.35	0.09	0.54	0.81	0.02	0.07	0.02		Bal.	337
AA7050-T76	0.03	0.06	2.1	0	2.2	0	6.2	0.02		Bal.	559
Ti6Al4V		<0.4						Bal.	3.5–4.5	5.5–6.75	>895

In contrast, for aluminium alloys of the 7xxx series welded to Ti, investigations are very scarce, all indicating some kind of limitation in terms of mechanical strength. Aonuma and Nakata (2011) compared friction stir butt welding of AA7075 as well as AA2024 to Ti and Ti6Al4V and found the joint strength of AA7075 joints to be generally lower. To increase the joint strength in FSLW of AA7075 to Ti6Al4V, Dias et al. (2023) added a macro form fit by extruding Al in pre-drilled holes within the Ti sheet during FSLW. The authors of this investigation (Grassel and Klusemann, 2025) recently published a study revealing the interface temperature in FSLW of AA7050 and Ti6Al4V to be above the Al solidus due to tool interaction with the Ti surface. Therefore, it can be concluded, that for firm joining of AA7xxx alloys to Ti either the process temperature has to be above the Al solidus or the Ti has to be activated by plastic deformation – which again results in temperatures above the Al solidus – both leading to solidification defects. To overcome this, Österreicher et al. (2024) applied post-weld heat-treatment and achieve up to 15 % increase in strength compared to the as-welded state, indicating an improvement of the joining interface.

It can be seen, that conflictive results are found between FSW of aluminium 6xxx and 7xxx series to Ti. Within this study, two commercial aluminium alloys, namely AA6082 and AA7050, were FSLW-welded to Ti6Al4V. The choice of these alloys was based on previous experience (Grassel and Klusemann, 2025) as well as industrial relevance of the respective materials. Process parameters were adjusted to achieve comparable thermal cycles during welding. To reveal differences in diffusion kinetics and phase agglomeration depending on the Al alloy system, both material combinations were post-weld heat-treated and analysed using SEM and EDS. Lap-shear-testing was performed on macroscopic scale showing the influence of post-weld heat-treatment on the global mechanical properties of the Al-interface-Ti-system. To separate the influence of the global Al properties (i.e. the softening in the HAZ) from the actual strength of the interface, tensile testing with special micro-specimens of the joining interface was conducted. This study firstly provides a direct comparison of the behaviour at the global and local scale of the two highly used Al alloy series 6xxx and 7xxx during joining to Ti, providing quantitative and comparable insights in their weldability to Ti as well as highlighting their contradictory thermo-mechanical behaviour.

Materials and methods

Sheets of commercially available aluminium alloys AA6082-T6 and AA7050-T76 have been welded to Ti6Al4V sheets in lap-joint configuration. The chemical composition and ultimate tensile strength (UTS) are listed in Table 1. All sheets had a thickness of 2 mm and a length of 500 mm. The overlap was chosen as 60 mm with Al on the top and advancing side, as presented in Fig. 1. Welds of 470 mm in length were produced with a tool consisting of a 15 mm scrolled flat shoulder and a 6 mm tri-flat conical probe of 2 mm length made of HOTVAR® tool steel. FSW was performed using a custom-build 3-axis gantry machine (Henry Loitz Robotik). The tilt angle of the tool axis was set to 1° of pointing of the tool tip towards the welding direction.

Welding parameters were chosen knowledge-based, resulting in similar interface temperatures of 520 °C during welding, determined via K-type thermocouples inserted into milled grooves at the Ti surface (Grassel and Klusemann, 2025), and a similar lap-shear strength (LSS) of 5700 N (380 N/mm) for both alloys determined in pre-tests. Welding speed was kept constant at 2.5 mm/s to ensure similar process times between the welding of both aluminium alloys. Rotational speed and axial force were chosen as 800 rpm, 4000 N for AA6082 and 1100 rpm, 8000 N for AA7050. Nine sections of 40 mm in width were cut out perpendicular to each weld using a wet separating machine before performing heat treatment using the samples in randomised order to avoid influence of the welding process.

Post-weld heat-treatment (HT) was performed at 120; 220; 320; and 420 °C for 6; 24 and 48 h, respectively. Temperatures were chosen to uniformly cover the temperature range between room temperature and the peak interface temperature during welding. Three specimens per alloy and HT procedure were inserted in a Nabertherm furnace. To reduce oxidation, sections were wrapped into aluminium foil before heat-treatment. Cooling of the samples was done at ambient condition. Heating and cooling times of the samples were adjusted by inserting them in sand prior to the heat-treatment. The sand acted as a heat reservoir, increasing the heating and cooling time to approximately 1 h.

After heat-treatment, sections for microscopic investigation and micro-tensile specimens as well as lap-shear specimens, see Fig. 2, were extracted using water-jet cutting. Quasi-static lap-shear tests were performed with specimens of 15 mm gauge width at a test-speed of 1 mm/min using a ZwickRoell universal testing machine. Micro-tensile specimens with a cross-section of 0.6 × 0.6 mm, as shown in Fig. 3, were eroded perpendicular to the interface at the weld centreline. This was done to eliminate the limiting effect of the heat-affected zone on the LSS and to reveal the interface properties. Micro-tensile tests were conducted using a Deben MT5000 micro tensile stage at a test-speed of 0.1 mm/min.

Cross-sections taken perpendicular to the welds were metallographically prepared using wet grinding, polishing with diamond suspension and oxide polishing suspensions. Cross-sections were investigated using SEM (Thermo Fisher Scientific Quanta 650 FEG) and EDS (AMETEK EDAX). A voltage of 10 kN and working distance of 10 mm was used to reveal interface morphology and chemical composition.

Results

Lap-shear testing

Fig. 4 gives an overview of the fracture behaviour of both AA6082 and AA7050 to Ti welds after HT at various temperatures during lap-shear testing. For AA6082, fracture occurred mainly in the HAZ despite after HT @ 220 °C, while for AA7050 fracture mainly occurred in the interface with the exception of HT @ 320 °C. Comparing the lap-shear force over HT time and temperature, see Fig. 5, it is noticeable that the influence of the HT time on the LSS is low compared to the influence of HT temperature. For AA6082 in as-welded condition as well as HT @ 120 °C, fracture occurred in the HAZ of the Al alloy at around 160 N/mm^2,[1] which implies that the actual lap-shear force of the interface has to be higher than the tensile strength of the softened aluminium in the HAZ as indicated by the arrows in Fig. 5. For HT @ 220 °C, the LSS decreased to 5000 N, corresponding to a maximum stress of 170 N/mm^2, where fracture occurred in the interface, indicating a weakening of the Al–Ti interface. The actual LSS of the interface cannot be directly derived from the load force as the

[1] Calculated from the maximum LS force divided by the Al cross sectional area (15 mm × 2 mm).

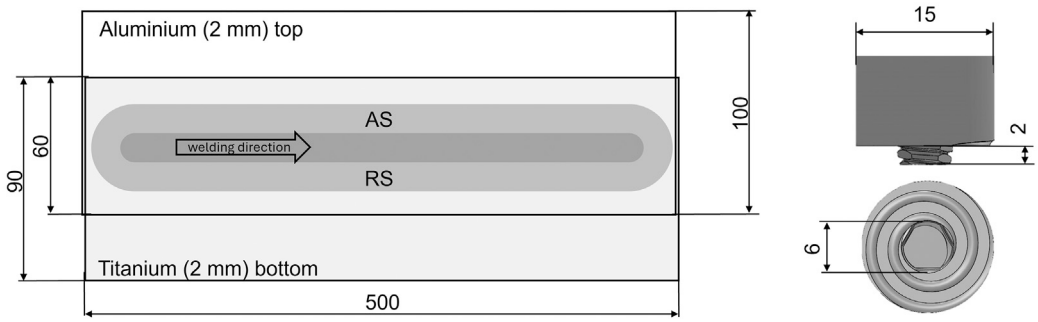

Fig. 1. Dimensions of welding setup showing overlap, welding direction, advancing side (AS) and retreating side (RS) as well as the FSW tool geometry. All dimensions in mm.

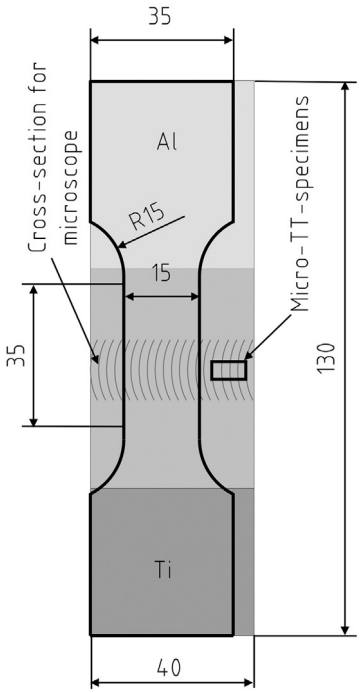

Fig. 2. Overview of heat-treated sample with extraction areas of specimens and position of the weld seam. From each HT sample, one lap-shear specimen as well as 3 micro-TT specimens, see dimensions in Fig. 3, within the weld region were extracted. All dimensions in mm.

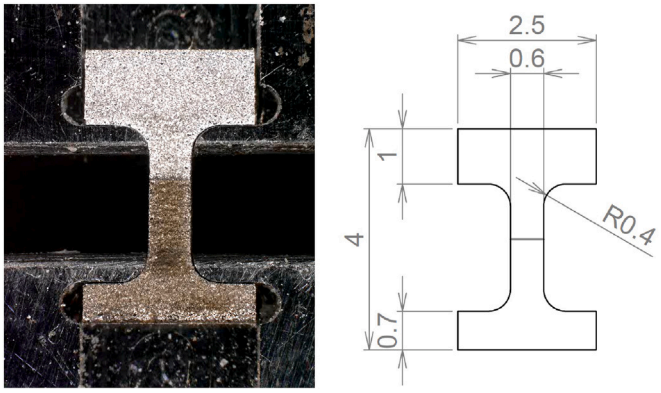

Fig. 3. Micro-tensile test specimen consisting of Al (light) and Ti (dark) inserted in test stage as well as relevant dimensions. All dimensions in mm.

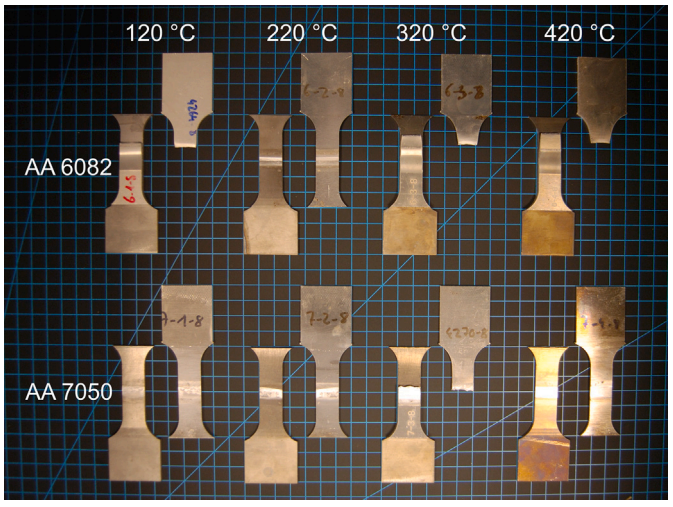

Fig. 4. Overview of fracture behaviour of lap- shear testing specimens of both Al alloys and HT temperatures showing mainly fracture in the Al HAZ for AA6082 and mainly fracture in the interface for AA7050.

width of the bonding zone is not exactly known. Based on observations of the fracture surface and results from other investigations (Chen and Nakata, 2009), the bonding width is in the range of the probe tip diameter and therefore between 5 and 6 mm, thus resulting in a LSS of around 70 N/mm^2. For higher HT temperatures, fracture occurred again in the HAZ at even lower forces because of softening of the Al caused by grain growth and dissolution of precipitates (Wagner et al., 2024). Regarding the influence of the HT time, highest LSS was reached at 24 h for HT @ 120 and 220 °C. Higher HT time as well as higher HT temperatures resulted in lower LSS due to the softening in the HAZ.

A completely different behaviour is observed for AA7050. Here, the LSS in as-welded condition and HT @ 120 °C are similar, see Fig. 6, where fracture occurred in the interface, see Fig. 4. For HT @ 220 °C and 320 °C the LSS increased, indicating interdiffusion and/or other effects such as reduction of residual stresses that leads to strengthening of the bond. For 320 °C the fracture occurred in the HAZ of the Al. Therefore, the actual LSS of the interface is assumed even higher than the maximum tensile stress in the softened Al at the point of fracture (220 N/mm^2). Behaviour changes again for HT @ 420 °C, where LSS is almost reduced to 50 % and fracture occurred in the interface, meaning a significant loss in bonding firmness. It is visible that higher HT times lead to a higher deviation in LSS and also in tendency to a lower LSS. Contradictory behaviour is solemnly seen for HT @ 220 °C, where LSS slightly increased over HT time. However, the influence of HT time is found to be neglectable for AA7050.

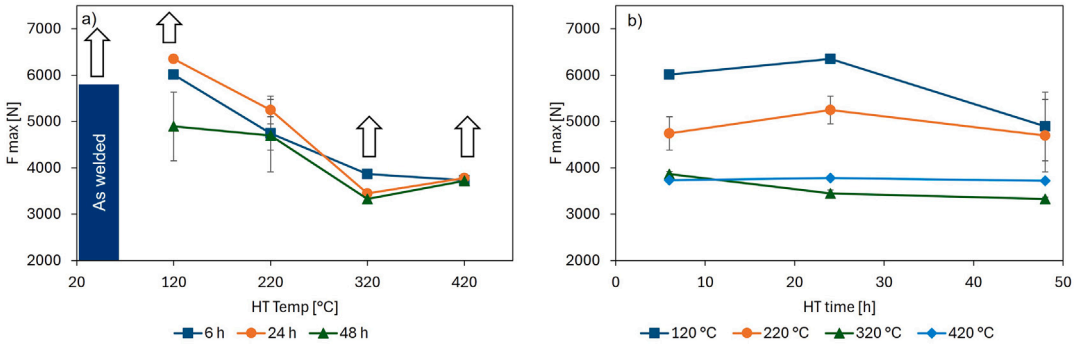

Fig. 5. Lap-shear force of AA6082-Ti6Al4V joints over (a) HT temperature and (b) time. Arrows indicate higher interfacial LSS than measured due to fracture in the Al HAZ.

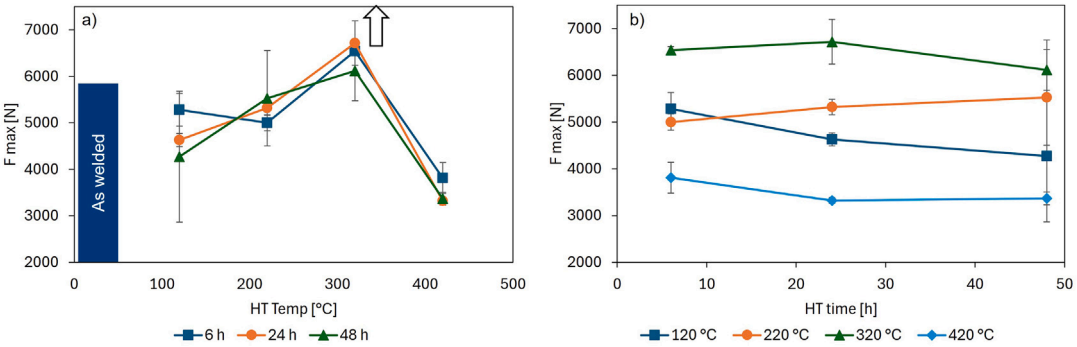

Fig. 6. Lap-shear strength of AA7050-Ti6Al4V joints over (a) HT temperature and (b) time. Arrow indicates higher interfacial LSS than measured due to fracture in the Al HAZ.

Micro tensile testing

As mentioned in the previous section, the meaningfulness of the lap-shear testing regarding the interface strength is limited by the failure in the Al HAZ. To overcome this issue, special micro-tensile specimens were designed and extracted from the weld centreline, see Fig. 2. Therefore, the micro-tensile specimens are designed to consist of Ti, the interface and Al from the stir zone, which is known to have higher mechanical strength than the HAZ for AA6082 (Costa et al., 2015) as well as AA7050 (Sun et al., 2018).

As the LSS results have shown little influence of HT time on the mechanical properties, micro-tensile testing (micro-TT) was performed only for HT times of 48 h. Compared to the lap-shear testing (Fig. 5), the micro-TT specimens for AA6082, see Fig. 7, show a differing behaviour over HT temperature. While LSS decreased from as-welded to HT @ 220 °C, then increased significantly at HT @ 320 °C and is lowest for HT @ 420 °C, for the micro-TT an almost constant strength was determined for the different HT temperatures, with highest strength (corresponding to 157 N/mm^2 UTS) for HT @ 220 °C. For HT temperatures of 320 °C and 420 °C, fracture occurred within the aluminium so that the actual tensile strength of the interface should be higher. The UTS and LSS values calculated from lap-shear and micro-TT testing are summarised in Table 2. It can be seen that at HT @ 220 °C and above, the calculated UTS values for both testing methods are in good agreement. For as-welded samples and HT @ 120 °C, the values are not directly comparable, as the fracture occurred in Al for the LSS and in the interface for the micro-TT samples. However, the results are matching, as the UTS value of the interface from the micro-TT is below the UTS of Al and above the maximum stress in LSS-testing.

For AA7050, the behaviours of the LSS (Fig. 6) and micro-TT (Fig. 7) follow a very similar trend with a maximum for HT @ 320 °C. Here, all specimens fractured in the interface so that the results represent the actual interface strength of the joints. The tensile strength increased by around 45 % from HT @ 220 °C to HT @ 320 °C, while the increase in LSS is only around 10 % due to the weakening in the HAZ, see Fig. 6. As the specimen cross-section was 0.6 × 0.6 mm^2, the maximum interface UTS can be calculated as 225 N/mm^2, see Table 2. Unfortunately, no micro-TT specimen of AA7050 could be tested in the as-welded state as these specimens fractured during the manufacturing process of the micro-TT samples, indicating a weak or brittle interface bonding. A direct comparison to the HT specimens is therefore not possible. Comparing the calculated UTS and LSS values of the interface, see Table 2, it can be noted that the calculated LSS values are around 50 % lower, thus indicating that the actual bonded area is respectively smaller (viz. 2.5 mm in width).

Interface structure

The microstructure at the interface was analysed via SEM for HT times of 48 h. For AA6082, a thin discontinuous layer in the interface is visible that grows with increasing HT temperature and reaches up to 250 nm after 48 h @ 420 °C, see Fig. 8. However, the interlayer is still not homogeneous. EDS line scanning over the interface, see Fig. 9, shows a chemical composition of about 25 % Ti and 75 % Al, corresponding to $TiAl_3$. But also Si concentration is found to be increased in this region.

For AA7050, a distinct interlayer is not obvious in the SEM micrographs, as shown in Fig. 10, however, the EDS line-scans, see Fig. 11, reveal a step in the concentration gradient from HT @ 220 °C on. Besides Ti and Al, this phase also contains a significant amount (up to 10 %) of Mg in a layer of 250–300 nm from the interface.

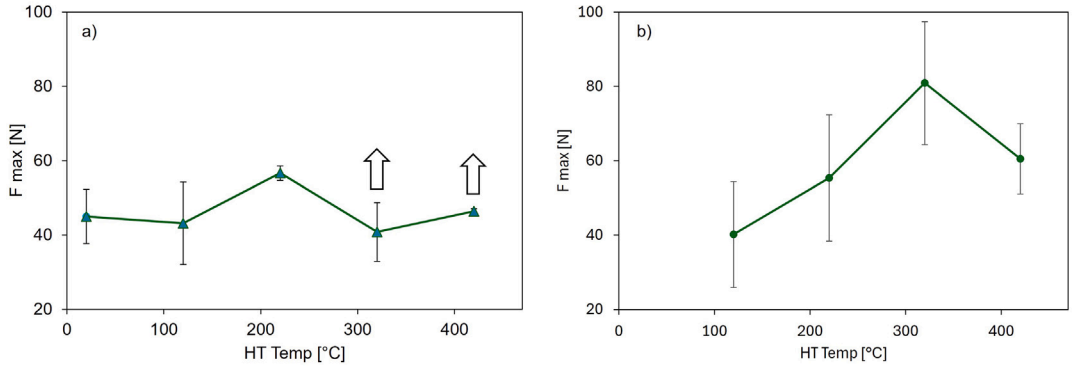

Fig. 7. Tensile strength of micro-TT specimens of (a) AA 6082 and (b) AA 7050 to Ti6Al4V joints over HT temperature for 48 h of HT time. Arrows indicate a higher interfacial strength than measured due to fracture in the Al.

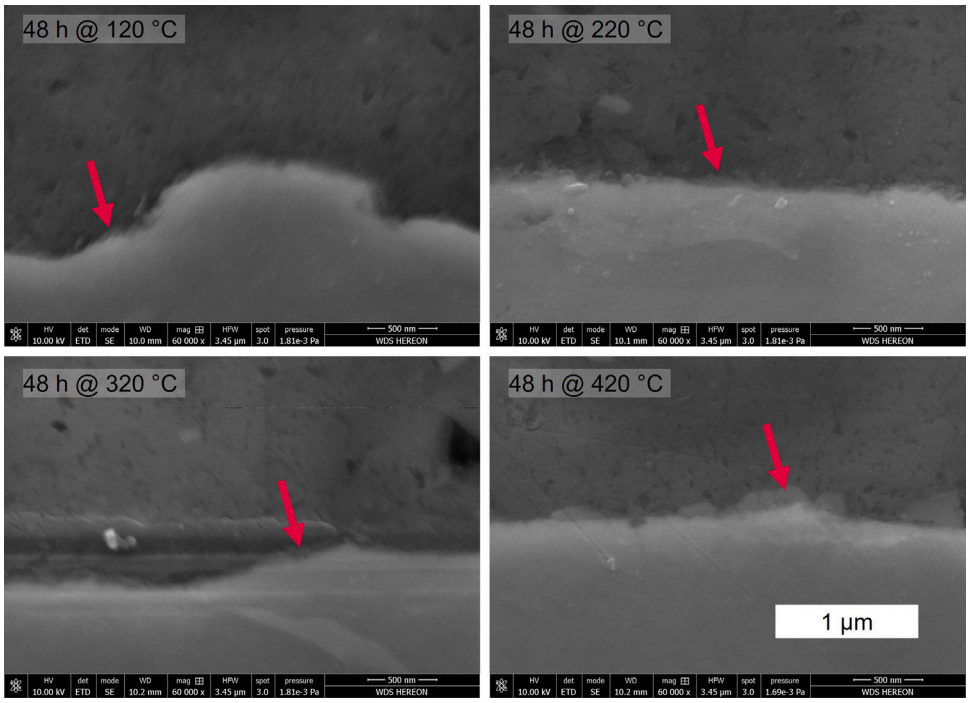

Fig. 8. SEM micrographs of the AA6082-Ti6Al4V interface after 48 h HT at various temperatures, arrows indicating growing discontinuous IMC layer reaching up to 250 nm thickness.

Table 2
Estimated values based on the fracture forces and cross-sectional areas for ultimate tensile strength of Al cross-section ($UTS_{Al\ Macro}$), lap-shear strength of the Al–Ti-interface ($LSS_{Al–Ti\ Macro}$) and ultimate tensile strength of the Al–Ti interface in micro-TT ($UTS_{Al–Ti\ Micro}$).

Material	HT Temp [°C]	HT time [h]	$UTS_{Al\ Macro}$ [N/mm²]	$LSS_{Al–Ti\ Macro}$ [N/mm²]	$UTS_{Al–Ti\ Micro}$ [N/mm²]
Cross-sectional area			15 × 2 mm²	15 × 5 mm²	0.6 × 0.6 mm²
	20		190	>76	125
	120		163	>65	120
6082	220		>156	63	157
	320		111	>44	>113
	420	48	124	>50	>129
	20		>188	75	–
	120		>142	57	112
7050	220		>184	74	154
	320		204	>82	225
	420		>112	45	168

Discussion

As the above results show, AA6082 to Ti and AA7050 to Ti welds react different to post-weld HT. The AA6082 to Ti6Al4V welds show high mechanical strength in the as-welded state, which is in accordance with findings in the literature (Krutzlinger et al., 2014). This high initial joint strength is believed to be caused by interdiffusion of Al and Ti as no indication of chemical reaction (IMC) of the joining partners could be found, see Fig. 9. Kalinenko et al. (2023) attributed the narrow diffusion zone to the low temperature in the Ti during welding due to the low thermal conductivity. In contrast, investigations by Fuji (2002) and Wilden and Bergmann (2004) showed silicon to hinder the diffusion of Al to Ti and to increase the diffusion temperature for a reliable joint by 40 K. However, in contrast to other researchers like Kalinenko et al. (2023), who found an increased concentration of silicon, manganese and magnesium in the interface, no significant enrichment was found in the present investigation in the as-welded state, see Fig. 9.

At HT temperatures between 120 and 220 °C a drastic decrease in LSS is found, which might be attributed to the formation of a

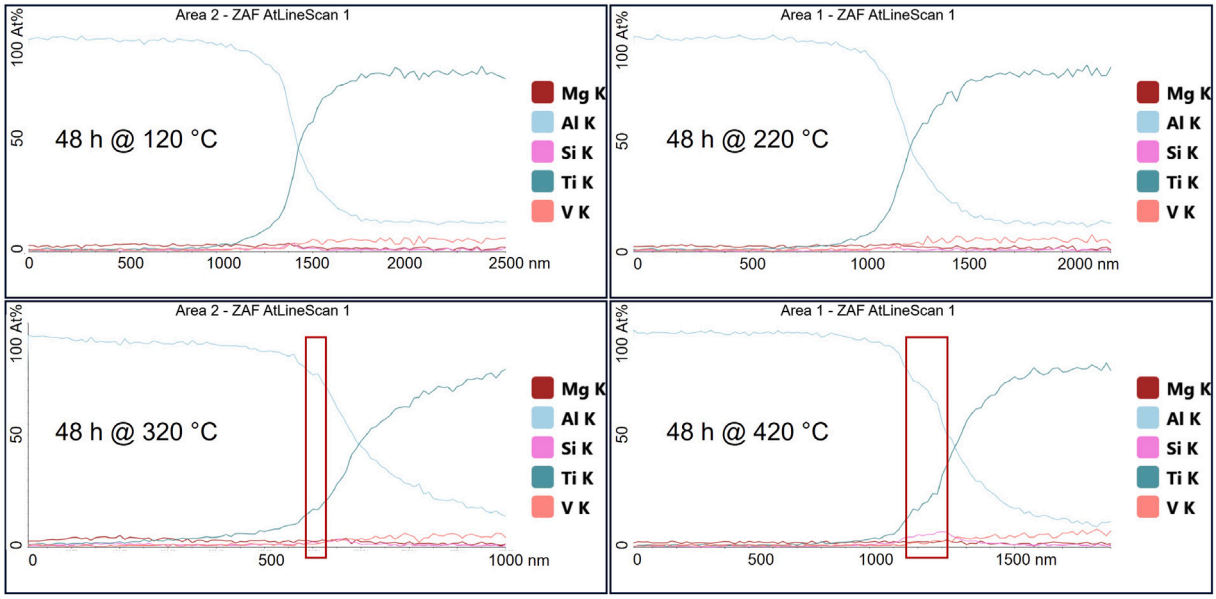

Fig. 9. EDS linescans over the AA6082-Ti6Al4V interface after 48 h HT at various temperatures, rectangles indicating IMC layers.

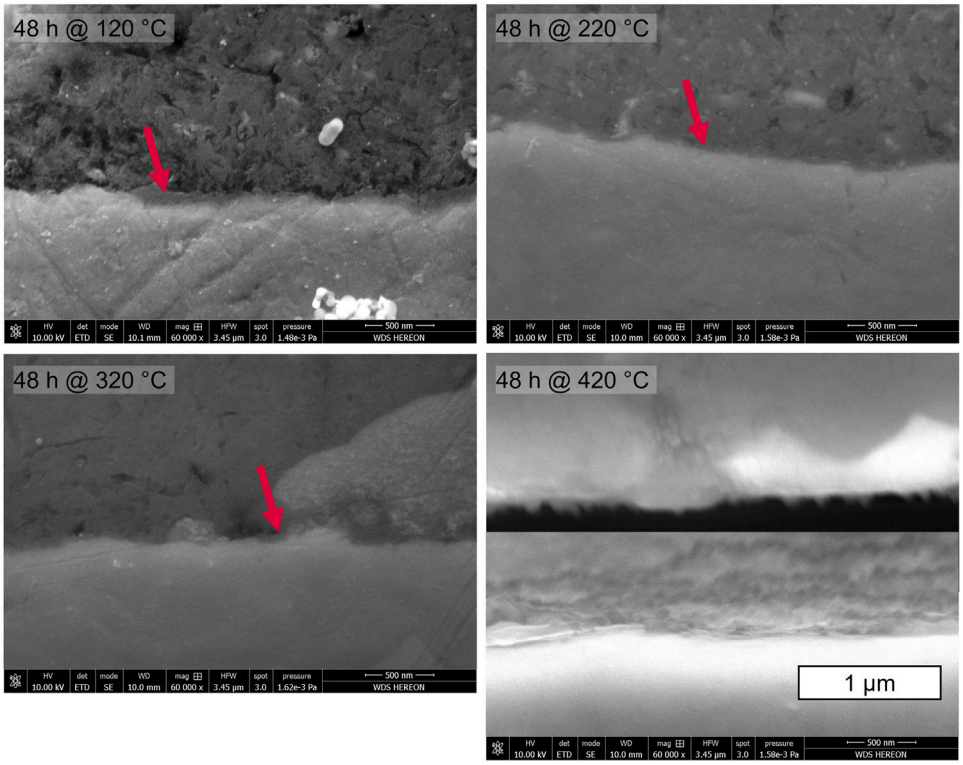

Fig. 10. SEM micrographs of the AA7050-Ti6Al4V interface after 48 h HT at various temperatures, arrows indicating possible IMC spots. The Sample HT @ 420 °C fractured during preparation, Al and Ti edge are shown respectively.

new discontinuous phase in the interface, see Fig. 9. However, it was not possible to identify this phase during EDS analysis. At higher HT temperatures, a distinct IMC layer, consisting of $Ti(Al,Si)_3$ (Gupta, 2002) is formed. Unfortunately, its influence on the mechanical properties cannot be evaluated in detail because of the premature fracture in Al during LSS and micro-TT testing. However, no detrimental effect is expected as the peak-stress in the interface did not decrease significantly.

It can be summarised that AA6082 to Ti welds show a high initial LSS, which is deteriorated by PWHT due to the softening of the Al, reducing the global mechanical properties. This indicates that an almost optimal interface composition is already reached during welding, where PWHT up to 220 °C has only a small effect on the interface strength.

The influence of PWHT on the AA7050 to Ti6Al4V welds was found significant at HT temperatures exceeding 120 °C. In contrast to the AlMgSi alloy AA6082, an increase in the global as well as local strength is visible with increasing HT temperature. This might be attributed to the higher amount of alloying elements, namely copper, magnesium and zinc. Tardy and Tu (1985) found copper addition to increase the activation energy for Ti diffusion and therefore reducing the formation

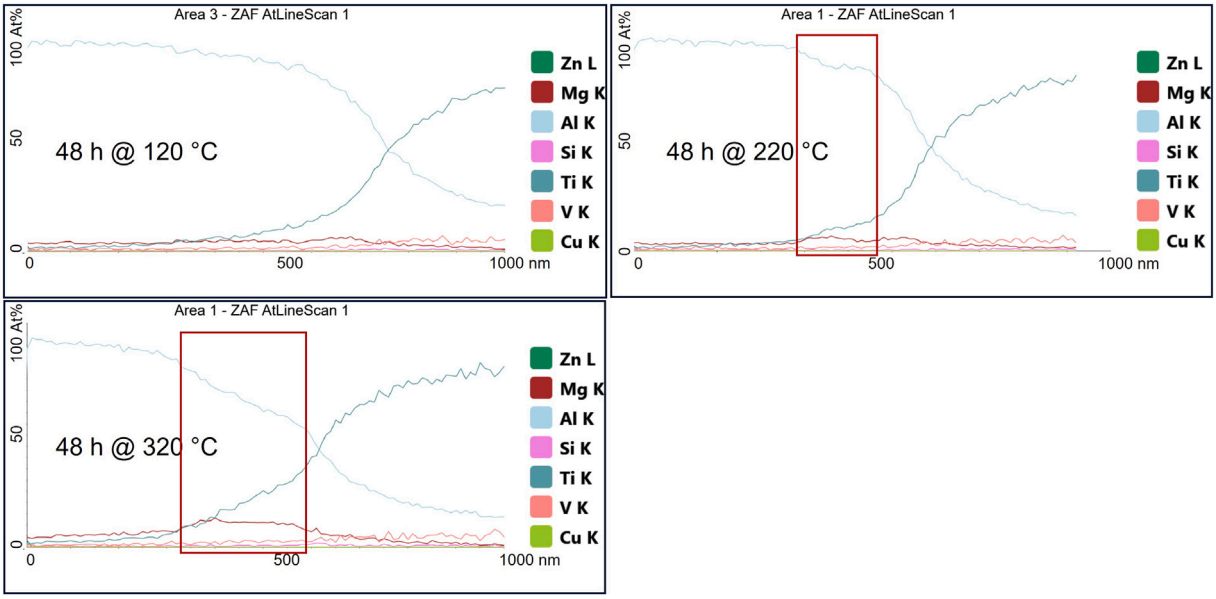

Fig. 11. EDS linescans over the AA7050-Ti6Al4V interface after 48 h HT at various temperatures, rectangles indicating IMC reaching up to 270 nm. No linescan could be taken at 420 °C because of sample fracture during preparation.

of $TiAl_3$. Additionally, Kar et al. (2019b) found Cu to absorb diffusing Al and Ti atoms forming Al–Cu and Ti–Cu IMCs. Similar behaviour is found for zinc, which forms IMC with Ti (Kar et al., 2019a) and therefore reduces the interaction of Ti and Al (Kar et al., 2018). However, in the present investigation, no agglomeration of Cu or Zn in the interface was detectable, see Fig. 11. Magnesium is known to accumulate in the interface, thus increasing the diffusion rate by up to 10 (Fuji et al., 2004) and lowering the minimum diffusion temperature for firm bonding by 40 K, respectively (Wilden and Bergmann, 2004; Wilden et al., 2006). Additionally, Ti, Mg and Al form IMCs, especially the τ-phase ($Al_{18}Mg_3Ti_2$) (Kurt et al., 2018), which is also found after PWHT of friction welded samples (Fuji et al., 2004). Analysing the EDS results in Fig. 11, an increase in Mg content is visible in the interface, which increases with increased HT temperature. At HT @ 320 °C, the chemical composition in the interface approaches the τ-phase. In this case, the highest strength is found, exceeding the as-welded state by about 40 %. Further increase of the HT temperature leads to a drastic loss in joint strength, possibly caused by the embrittlement due to the growth of the τ-phase. It was not possible to correlate this behaviour to the chemical composition as the samples repeatedly fractured during preparation, see Fig. 10.

In summary, the results show that for FSW of AA7050 to Ti, the interface is not in the optimum condition directly after welding. PWHT allows for further interdiffusion with beneficial effects on the joint strength. The optimum HT temperature has been found to be in the range of 320 °C. Above this temperature, deterioration of the LSS, similar to the AA6082 welds, was found.

Conclusion

The influence of PWHT on two commercially Al alloys (AA6082 and AA7050) friction stir welded with Ti6Al4V was analysed regarding mechanical properties and interfacial diffusion. For both alloy combinations, contrary evolution of the Al and the interface strength is found. It can therefore be stated, that improving the strength of Al alloys to Ti FSW welds by proper application of PWHT is possible but strongly dependent on the alloy composition. Furthermore, the following conclusions can be drawn:

1. PWHT shows significant influence on LSS of Al–Ti FSW lap-joints above 120 °C HT temperature.
2. At the applied PWHT conditions, the influence of the PWHT time is insignificant compared to the PWHT temperatures.
3. An increase on joint strength of AA7050 to Ti6Al4V by up to 40 % could be achieved by PWHT at 320 °C.
4. Alloying elements in Al have significant influence on the diffusion behaviour of Al and Ti. While AlMgSi alloys show a faster diffusion behaviour resulting in firm bonding directly after welding, AlCuZn alloys show lower diffusion kinetics, resulting in an increase in bond strength during PWHT up to 320 °C.
5. While Mg and Si are the only two alloying elements found to agglomerate in the interface, Mg is believed to have the most significant influence on the diffusion kinetics as it agglomerates in the interface and forms a compound with Al and Ti.

CRediT authorship contribution statement

Felix Grassel: Writing – review & editing, Writing – original draft, Visualization, Methodology, Investigation, Data curation, Conceptualization. **Benjamin Klusemann:** Writing – review & editing, Supervision, Methodology, Funding acquisition, Conceptualization.

Declaration of competing interest

The authors declare that they have no known competing financial interests or personal relationships that could have appeared to influence the work reported in this paper.

Acknowledgments

Funding by the Deutsche Forschungsgemeinschaft (DFG, German Research Foundation), Germany – project number 464986536 - is gratefully acknowledged.

Data availability

The obtained data of this research is online available at Zenodo (10.5281/zenodo.19559286).

References

Aonuma, M., Nakata, K., 2011. Dissimilar metal joining of 2024 and 7075 aluminium alloys to titanium alloys by friction stir welding. Mater. Trans. (ISSN: 1345-9678) 52 (5), 948–952. http://dx.doi.org/10.2320/matertrans.L-MZ201102.

Beygi, R., Galvão, I., Akhavan-Safar, A., Pouraliakbar, H., Fallah, V., da Silva, L.F.M., 2023. Effect of alloying elements on intermetallic formation during friction stir welding of dissimilar metals: A critical review on aluminum/steel. Metals 13 (4), 768. http://dx.doi.org/10.3390/met13040768, PII: met13040768.

Chen, Y.C., Nakata, K., 2009. Microstructural characterization and mechanical properties in friction stir welding of aluminum and titanium dissimilar alloys. Mater. Des. (ISSN: 02613069) 30 (3), 469–474. http://dx.doi.org/10.1016/j.matdes.2008.06.008, PII: S0261306908002641.

Chen, Z.W., Yazdanian, S., 2015. Microstructures in interface region and mechanical behaviours of friction stir lap Al6060 to Ti–6Al–4V welds. Mater. Sci. Eng.: A (ISSN: 09215093) 634, 37–45. http://dx.doi.org/10.1016/j.msea.2015.03.017, PII: S0921509315002361.

Costa, M.I., Rodrigues, D.M., Leitão, C., 2015. Analysis of AA 6082-T6 welds strength mismatch: stress versus hardness relationships. Int. J. Adv. Manuf. Technol. (ISSN: 0268-3768) 79 (5–8), 719–727. http://dx.doi.org/10.1007/s00170-015-6866-z, PII: 6866.

Dias, F., Cipriano, G., Correia, A.N., Braga, D.F.O., Moreira, P., Infante, V., 2023. Joining of aluminum alloy AA7075 and titanium alloy Ti-6Al-4V through a friction stir welding-based process. Metals 13 (2), 249. http://dx.doi.org/10.3390/met13020249, PII: met13020249.

Dressler, U., Biallas, G., Alfaro Mercado, U., 2009. Friction stir welding of titanium alloy TiAl6V4 to aluminium alloy AA2024-T3. Mater. Sci. Eng.: A (ISSN: 09215093) 526 (1–2), 113–117. http://dx.doi.org/10.1016/j.msea.2009.07.006, PII: S0921509309007515.

Fuji, A., 2002. In situ observation of interlayer growth during heat treatment of friction weld joint between pure titanium and pure aluminium. Sci. Technol. Weld. Join. (ISSN: 1362-1718) 7 (6), 413–416. http://dx.doi.org/10.1179/136217102225006903.

Fuji, A., Ikeuchi, K., Sato, Y.S., Kokawa, H., 2004. Interlayer growth at interfaces of Ti/Al–1%Mn, Ti/Al–4.6%Mg and Ti/pure Al friction weld joints by post-weld heat treatment. Sci. Technol. Weld. Join. (ISSN: 1362-1718) 9 (6), 507–512. http://dx.doi.org/10.1179/136217104225021797.

Grassel, F., Klusemann, B., 2025. Friction stir lap weld-brazing of AA7050 aluminium alloy to Ti6Al4V titanium alloy – Limitations in dissimilar metal joining. Manuf. Lett. (ISSN: 22138463) 44, 37–41. http://dx.doi.org/10.1016/j.mfglet.2025.03.005, PII: S2213846325000136.

Grassel, F., Malaske, L., Hoffmann, M., Klusemann, B., 2025. (Semi-)solid-state joining of aluminium and titanium alloys – a critical review. J. Mater. Res. Technol. (ISSN: 22387854) 39, 3270–3291. http://dx.doi.org/10.1016/j.jmrt.2025.09.239, PII: S2238785425024937.

Gupta, S.P., 2002. Intermetallic compounds in diffusion couples of Ti with an Al-Si eutectic alloy. Mater. Charact. (ISSN: 10445803) 49 (4), 321–330. http://dx.doi.org/10.1016/S1044-5803(02)00342-X, PII: S104458030200342X.

Haghshenas, M., Khodabakhshi, F., 2019. Dissimilar friction-stir welding of aluminum and polymer: a review. Int. J. Adv. Manuf. Technol. (ISSN: 0268-3768) 104 (1–4), 333–358. http://dx.doi.org/10.1007/s00170-019-03880-2, PII: 3880.

Isa, M.S.M., Moghadasi, K., Ariffin, M.A., et al., 2021. Recent research progress in friction stir welding of aluminium and copper dissimilar joint: a review. J. Mater. Res. Technol. (ISSN: 22387854) 15, 2735–2780. http://dx.doi.org/10.1016/j.jmrt.2021.09.037, PII: S2238785421010188.

Kalinenko, A., Dolzhenko, P., Borisova, Y., Malopheyev, S., Mironov, S., Kaibyshev, R., 2022. Tailoring of dissimilar friction stir lap welding of aluminum and titanium. Mater. (Basel, Switzerland) (ISSN: 1996-1944) 15 (23), http://dx.doi.org/10.3390/ma15238418, Journal Article The authors declare no conflict of interest..

Kalinenko, A., Dolzhenko, P., Malopheyev, S., et al., 2023. Interfacial microstructure produced during dissimilar AA6013/Ti-6Al-4V friction stir lap welding under zero-penetration condition. Metals 13 (10), 1667. http://dx.doi.org/10.3390/met13101667, PII: met13101667.

Kar, A., Kailas, S.V., Suwas, S., 2018. Effect of zinc interlayer in microstructure evolution and mechanical properties in dissimilar friction stir welding of aluminum to titanium. J. Mater. Eng. Perform. (ISSN: 1059-9495) 27 (11), 6016–6026. http://dx.doi.org/10.1007/s11665-018-3697-8, PII: 3697.

Kar, A., Suwas, S., Kailas, S.V., 2019a. Microstructural modification and high-temperature grain stability of aluminum in an aluminum-titanium friction stir weld with zinc interlayer. JOM (ISSN: 1047-4838) 71 (1), 444–451. http://dx.doi.org/10.1007/s11837-018-3152-1, PII: 3152.

Kar, A., Suwas, S., Kailas, S.V., 2019b. Significance of tool offset and copper interlayer during friction stir welding of aluminum to titanium. Int. J. Adv. Manuf. Technol. (ISSN: 0268-3768) 100 (1–4), 435–443. http://dx.doi.org/10.1007/s00170-018-2682-6, PII: 2682.

Krutzlinger, M., Marstatt, R., Suenger, S., Luderschmid, J., Zaeh, M.F., Haider, F., 2014. Formation of joining mechanisms in friction stir welded dissimilar al-ti lap joints. Adv. Mater. Res. 966–967, 510–520. http://dx.doi.org/10.4028/www.scientific.net/AMR.966-967.510.

Kurt, H.I., Guzelbey, I.H., Salman, S., 2018. An experimental study of investigating the relationships between structures and properties of al alloys included with high Mg and high Ti. Int. J. Mater. Prod. Technol. (ISSN: 0268-1900) 56 (3), 271. http://dx.doi.org/10.1504/IJMPT.2018.090819.

Mishra, R.S., Ma, Z.Y., 2005. Friction stir welding and processing. Mater. Sci. Eng.: R: Rep. (ISSN: 0927796X) 50 (1–2), 1–78. http://dx.doi.org/10.1016/j.mser.2005.07.001, PII: S0927796X05000768.

Österreicher, J.A., Pfeiffer, C., Kunschert, G., et al., 2024. Dissimilar friction stir welding and post-weld heat treatment of Ti-6Al-4V and AA7075 producing joints of unprecedented strength. J. Adv. Join. Process. (ISSN: 26663309) 9 (5), 100213. http://dx.doi.org/10.1016/j.jajp.2024.100213, PII: S2666330924000293.

Rostami, H., Nourouzi, S., Jamshidi Aval, H., 2018. Analysis of welding parameters effects on microstructural and mechanical properties of Ti6Al4V and AA5052 dissimilar joint. J. Mech. Sci. Technol. (ISSN: 1738-494X) 32 (7), 3371–3377. http://dx.doi.org/10.1007/s12206-018-0640-8, PII: 640.

Simar, A., Avettand-Fènoël, M.-N., 2017. State of the art about dissimilar metal friction stir welding. Sci. Technol. Weld. Join. (ISSN: 1362-1718) 22 (5), 389–403. http://dx.doi.org/10.1080/13621718.2016.1251712.

Sun, T., Reynolds, A.P., Roy, M.J., Withers, P.J., Prangnell, P.B., 2018. The effect of shoulder coupling on the residual stress and hardness distribution in AA7050 friction stir butt welds. Mater. Sci. Eng.: A (ISSN: 09215093) 735, 218–227. http://dx.doi.org/10.1016/j.msea.2017.12.018, PII: S0921509317316155.

Tardy, J., Tu, K.N., 1985. Solute effect of Cu on interdiffusion in Al3Ti compound films. Phys. Rev. B (ISSN: 0163-1829) 32 (4), 2070–2081. http://dx.doi.org/10.1103/PhysRevB.32.2070, Journal Article.

Thomas, W.M., Nicholas, E.D., Needham, J.C., Murch, M.G., Temple, S.P., Dawes, C.J., 1995. Friction welding. US5460317 (A).

Wagner, D., Bernardi, M., Grassel, F., et al., 2024. Analysis of mechanical properties and microstructure of single and double-pass friction stir welded T-joints for aluminium stiffened panels. Mater. Des. (ISSN: 02613069) 247, 113438. http://dx.doi.org/10.1016/j.matdes.2024.113438.

Wei, Y., Li, J., Xiong, J., Huang, F., Zhang, F., Raza, S.H., 2012. Joining aluminum to titanium alloy by friction stir lap welding with cutting pin. Mater. Charact. (ISSN: 10445803) 71 (1–2), 1–5. http://dx.doi.org/10.1016/j.matchar.2012.05.013, PII: S1044580312001519.

Wilden, J., Bergmann, J.P., 2004. Manufacturing of titanium/aluminium and titanium/steel joints by means of diffusion welding. Weld. Cut. 56 (5), 285–290.

Wilden, J., Bergmann, J.P., Jahn, S., 2006. Mechanical properties and processing of low-temperature diffusion-welded hybrid joints. Adv. Eng. Mater. (ISSN: 1438-1656) 8 (3), 212–218. http://dx.doi.org/10.1002/adem.200600006.

Wu, A., Song, Z., Nakata, K., Liao, J., Zhou, L., 2015. Interface and properties of the friction stir welded joints of titanium alloy Ti6Al4V with aluminum alloy 6061. Mater. Des. (ISSN: 02613069) 71 (Part A), 85–92. http://dx.doi.org/10.1016/j.matdes.2014.12.015, PII: S0261306914009972.

Yu, M., Zhao, H., Jiang, Z., et al., 2019. Influence of welding parameters on interface evolution and mechanical properties of FSW Al/Ti lap joints. J. Mater. Sci. Technol. (ISSN: 10050302) 35 (8), 1543–1554. http://dx.doi.org/10.1016/j.jmst.2019.04.002, PII: S1005030219300908.